Effects on vibrational and electronic properties of removing hydrogen atoms in hydrogenated amorphous silicon

J. S. Nelson and C. Y. Fong
Department of Physics, University of California, Davis, California 95616

L. Guttman
Materials Science Division, Argonne National Laboratory, Argonne, Illinois 60439-4843

Inder P. Batra
IBM Almaden Research Center (Mail Stop K33/801), 650 Harry Road, San Jose, California 95120-6099

(Received 23 April 1987)

The effects of removing hydrogen atoms on the vibrational and the electronic properties of hydrogenated amorphous silicon (*a*-Si:H) have been investigated. Besides the missing vibrational modes associated with the removal of H atoms, the changes in the Si-dominated modes can be correlated to local distortions at the site of the Si whose neighboring H was removed. The dangling-bond states have an average energy at 0.2 eV above the top of the valence band, which is 0.5 eV smaller than the generally accepted value for the electronic level with $g = 2.0055$. The range of interaction between the dangling-bond states is about equal to the second-neighbor distance (≤ 4 Å). Comparison of the electronic states with and without the presence of the hydrogen atoms allows us to locate the Si—H bonding states at 5.0 and 7.5 eV below the top of the valence band.

I. INTRODUCTION

Since the suggestion made by Paul, Lewis, Connell, and Moustakas[1] that the presence of hydrogen atoms is a crucial factor for possible doping in amorphous silicon (*a*-Si), studies of the basic vibrational and electronic properties for hydrogenated amorphous silicon (*a*-Si:H) have been carried out by many research groups. The infrared spectrum has been measured by Shen *et al.*,[2] who found, in addition to the absorption in *a*-Si at frequencies below 500 cm^{-1}, four prominent H-related peaks at 2090, 1985, 840, and 630 cm^{-1}. Photoemission measurements of *a*-Si:H by von Roedern *et al.*[3] on sputtered samples show four maxima in the valence-band density of states with binding energies of 2.4, 5.2, 7.4, and 10.5 eV. These authors identified the 5.2-eV maximum, the so-called *C* peak, and the 7.4-eV maximum, the *D* peak, with Si $3p$–H $1s$ and Si $3s$–H $1s$ states, respectively, for bonding single H atoms to Si (monohydride configuration) in *a*-Si:H. The results also show a recession of the top of the valence band (VB) in *a*-Si:H as compared to *a*-Si.

In regards to theoretical studies, the coherent-potential approximation (CPA) method has been applied to calculate the vibrational density of states (VDOS) of *a*-Si:H by Barrio *et al.*[4] Lattice dynamics calculations using periodic network models of *a*-Si:H have also been reported by some of us.[5] Besides the low-frequency vibrations of silicon atoms, all of the theoretical spectra have shown H-atom wagging modes at 680 cm^{-1} and Si—H stretching modes around 2100 cm^{-1}.[5,6]

The electronic density of states (EDOS) of *a*-Si:H has been calculated by Ching *et al.*[7] using the tight-binding method. The self-consistent pseudopotential method has been applied to periodic models of *a*-Si:H by Guttman and Fong;[8] they found that the valence EDOS associated with the hydrogen atoms in monohydride configurations shows maxima at 2.0, 5, 7.5, and 11.5 eV below the VB edge. Allan and Joannopoulos[9] investigated the EDOS of different configurations of hydrogen atoms in *a*-Si by using the cluster–Bethe-lattice method. They attributed the value of -4.6 eV to the monohydride contribution to the EDOS. Diaz *et al.*[10] reported Hartree-Fock self-consistent cluster–Bethe-lattice results; the Si—H bonding state appeared at -4.5 eV. Gap states were studied using the CPA method by Economou and Papaconstantopoulos,[11] who showed that the effect of the H atoms in *a*-Si is to widen the gap.

We report in this paper the effects of removing H atoms on the vibrational and the electronic properties of

TABLE I. Summary of the values of parameters used in Eq. (1).

α (10^5 dyn/cm)	β/α	$d_{\text{Si—Si}}$ (Å)	$d_{\text{Si—H}}$ (Å)	$\alpha_{\text{Si—H}}/\alpha$	$\gamma/\alpha d^8_{\text{Si—H}}$
0.48	0.15[a]	2.35	1.48	1.8[b]	0.0053

[a]Reference 15.
[b]Reference 16.

TABLE II. Parameters of the ionic pseudopotentials of Si^{4+} and H^+. a_0: Bohr radius.

Parameters	Si^{4+}	H^+
a_1 (Ry/a_0^2)	-1.167	0.351
a_2 ($1/a_0$)	0.791	0.280
a_3	-0.352	-1.538
a_4 $(1/a_0)^4$	-0.018	-0.007

a-Si:H. After the removal of a H atom from its neighboring Si atom, the Si atom will be at a threefold coordinated site. One of its electrons will not form a bond with any other atom; the term "dangling bond" or "T_3^0 level" is usually applied to this electronic state. By comparing the results before and after removing H atoms, we can study: (i) the changes in the vibrational and the electronic properties of a-Si:H, (ii) how these changes depend on the local environment at the Si atom; (iii) the electronic properties of the dangling bond and their dependence on the local environment; (iv) the range of interaction between the dangling bonds. It turns out that such comparisons enable us to determine the Si—H bonding states in the monohydride configuration. The results agree well with the experimental identification. The lattice dynamics and the self-consistent pseudopotential methods are applied to periodic random networks in monohydride configurations. A brief report has been given by Nelson *et al.*[12] In Sec. II, we present the methods. Results and discussion are given in Sec. III.

II. METHODS

The present calculations are based on two examples of random network models of a-Si:H and on a number of related examples obtained by the removal of hydrogen atoms to generate threefold coordinated Si atoms. We have assumed that the vibrational and the electronic states of this material are largely determined by short-range forces and that the effects of these states induced by a small structural change can be understood by examination of the immediate vicinity of that change. This assumption is almost guaranteed to be true for the vibrational states by the form of our assumed interatomic potential function. That it is true for the electronic states as well may be justified *a posteriori* by our success in interpretation

A. The models

The method of construction of the models has been described previously.[13] The two basic examples contained 54 Si atoms and six H atoms in the representing unit. No more than one H atom was bonded to any Si atom and no two H atoms were closer than fourth neighbors, in order to minimize H—H interactions. Models derived by removal of one or more H atoms were relaxed to the minimum energy configurations using the potential given in Sec. II B.

B. Vibrational spectrum

Since the models are periodic, the eigenvalues and eigenvectors of the vibrational modes were calculated, as usual, by diagonalizing the dynamical matrix. The potential was a modified version[13] of the Keating potential,[14]

$$V=\frac{3}{16}\sum_{i}^{\text{bonds}}\frac{\alpha_i}{d_i^2}(r_i^2-d_i^2)^2+\frac{3}{8}\sum_{i,j}^{\text{pairs}}{}'\frac{\beta_{ij}}{d_{ij}}(\bar{r}_i\cdot\bar{r}_j+\tfrac{1}{3}d_{ij}^2)^2+\sum_{\text{Si—H}}{}'\frac{\gamma}{r_{\text{Si—H}}^6}\,, \quad (1)$$

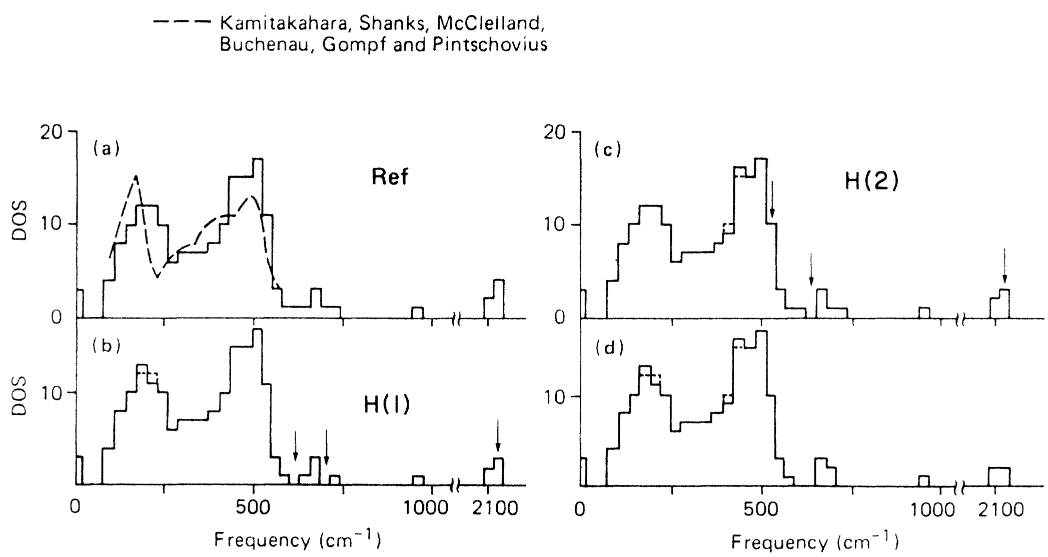

FIG. 1. Vibrational density of states of one random network a-Si:H compared to neutron data of a-Si. The calculated result serves as reference for (b)–(d). (b) H(1) removed (solid line), the reference is shown as a dashed line. (c) H(2) removed (solid line). (d) H(1) and H(2) removed (solid line).

where α_i and β_{ij} are the bond stretching and bending force constants. d_i is the equilibrium bond length (2.35 Å if the pair is two Si atoms, 1.48 Å if one is an H atom). d_{ij} is the product of d_i and d_j. $\bar{r}_i$ is an interatomic vector. The last term acts only between H and Si atoms not directly bonded and is necessary to prevent collapse of the network around the H atoms. The values of these constants are given in Table I. The same β value is used for all pairs of interatomic vectors, whether or not one joins Si to H.

C. Electronic spectrum

The self-consistent pseudopotential method has been described in many places.[8,17] The input ionic pseudopotentials of Si^{4+} and H^{+} are given by the following expression with the constants listed in Table II:

$$V(G)=a_1G^{-2}[\cos(a_2G)+a_3]e^{a_4G^4}, \tag{2}$$

where G is the magnitude of the reciprocal-lattice vector. The potentials were cut off at $G=4$ a.u. to match the inverse Fourier transforms to the known real-space pseudopotentials. In the present calculations, we used about 400 plane waves and included about another 100 plane waves in the Löwdin perturbation scheme.

III. RESULTS AND DISCUSSION

A. Vibrational properties

In Fig. 1(a) the vibrational density of states of one random network model is compared to that measured by neutron inelastic scattering of a-Si.[18] It will serve as a reference spectrum for the following discussion. The calculated major maxima due to the bond bending and stretching modes agree reasonably well with the experimental results. The two maxima between $250 \leq \omega \leq 450$ cm^{-1} shown in the experimental curve are not accounted for by the theory. The modes associated with these two structures have been discussed by Nichols *et al.*[19] At higher frequencies (>500 cm^{-1}), the theory gives two bands at 680 and 2100 cm^{-1}, the H-atom wagging and the H—Si stretching modes, as shown below. Their positions agree quite well with the infrared (ir) results.[2]

When one of the H atoms, labeled H(1), is removed from the model, the VDOS becomes that shown in Fig. 1(b) by the solid line. Three modes disappear, two having frequencies near 650 cm^{-1} and one with frequency in the neighborhood of 2100 cm^{-1}, as indicated by the arrows. But besides these changes, the Si-dominated modes show slight changes in the bond bending region as compared to the reference spectrum (dashed line). In Fig. 1(c), we show the VDOS when H(1) is restored while another H atom [labeled H(2)] is removed. Atom H(2) does not have any second neighbor in common with H(1). Again, three modes closely related to hydrogen motions disappear, and other small changes occur, mostly in the Si—Si bond stretching region. Finally [Fig. 1(d)], both H(1) and H(2) are removed. The changes in the Si-dominated bond bending and stretching regions are clearly additive.

To characterize the modes associated with H(1), we plot the corresponding eigenvector components in Fig. 2.

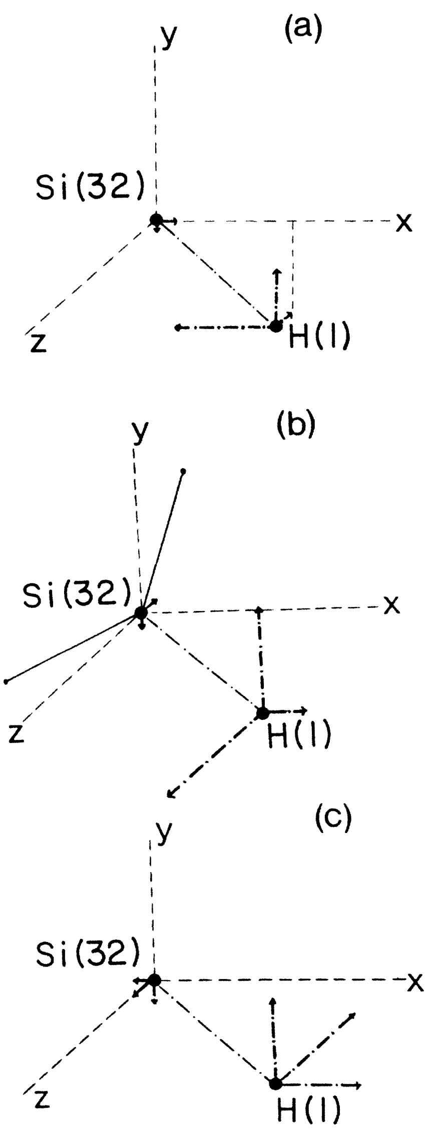

FIG. 2. (a) The missing Si(32)—H(1) stretching mode in Fig. 1(b) with respect to the result in Fig. 1(a). (b) The missing wagging mode of H(1) in Fig. 1(b). (c) The other missing wagging mode of H(1) in Fig. 1(b).

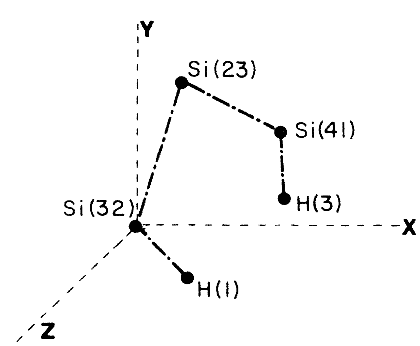

FIG. 3. The configuration between H(1) and H(3).

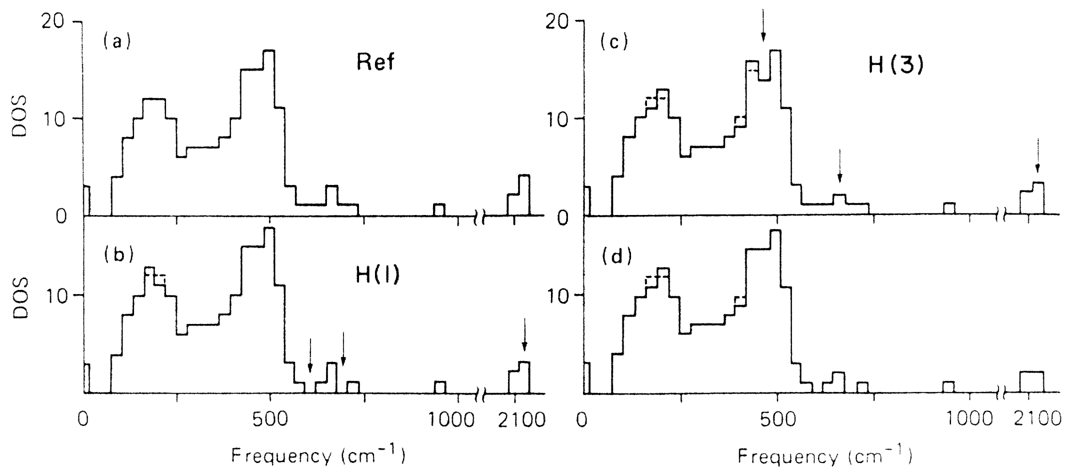

FIG. 4. (a) The reference vibrational density of states. (b) H(1) removed (solid line), the reference is shown as a dashed line. (c) H(3) removed (solid line). (d) H(1) and H(3) removed (solid line).

In Fig. 2 the atom Si(32), the nearest neighbor of H(1), is located at the origin. H(1) is below the X-Z plane with coordinate components $x > y > z$. Because the modes are localized, the other amplitudes except the first neighbor Si [Si(32)] are too small to show on the graph. The components of the eigenmode with a frequency at 2130 cm^{-1} are shown in Fig. 2(a). The motion of H(1) is along the bond Si(32)—H(1). In Figs. 2(b) and 2(c) (the 680-cm^{-1} modes) one sees that the H-atom motion is mainly perpendicular to the Si(32)—H bond. These modes are therefore the stretching and the wagging modes, respectively.

The additive behavior of the changes in the Si atom dominated modes can be attributed to the separation of H(1) and H(2) being greater than the range of the potential used in the calculations. For confirmation, we calculated the VDOS with H(1) and H(3) removed, where H(3) does have a second neighbor [Si(23)] in common with H(1). The geometric configuration is schematically shown in Fig. 3. The Si atoms and the H atoms are explicitly marked. H(3) is above the X-Z plane but behind the X-Y plane. The reference VDOS and that for the cases with H(1), H(3), and both H(1) and H(3) removed are shown in Fig. 4. By comparing the results of Fig. 4(d) to Figs. 4(a)–4(c), one sees that the changes of the VDOS in the region $\omega \leq 500$ cm^{-1} and with both H(1) and H(3) removed cannot be obtained by linearly superimposing the results with one H atom removed. The interaction range is about the second-neighbor distance ($\lesssim 4$ Å).

From the results shown in Figs. 2 and 4, it is obvious that one should ask the following question: Why do the changes in the Si-dominated modes happen in the bond bending region in some cases, while in others they occur in the bond stretching region? We relate the origin of these changes to the local environments at the Si atoms from which the H atoms are removed. In Table III we list for the three cases: (i) the nature of the changes in the Si-dominated modes, (ii) the average bond angle at the Si atom, and (iii) the most distorted bond length between the threefold coordinated Si atom and its three neighbors. The percentage deviations of the average bond angle and the shortest bond length from the ideal values are shown in parentheses. Because the angular distortion at Si(32) is larger than 5%, the corresponding change happens in the bond bending modes. On the other hand, when the bond length distortion at the Si atom neighboring to H(2) is equal to 5%, the stretching modes exhibit changes. Finally, the removal of H(3) causes changes in both the bending and stretching modes because its neighboring Si site has both angular and bond length distortions larger than 5%. Thus a correla-

TABLE III. Correlation between local environments and changes in Si-dominated vibrational modes.

Removed atom	Changes in Si-dominated modes	Average bond angle	Most distorted bond length (Å)
H(1)	bending	118° (8%)	2.312 (−1.6%)
H(2)	stretching	105.6° (−3.1%)	2.237 (−5%)
H(3)	bending and stretching	114.4° (5%)	2.085 (−11.3%)

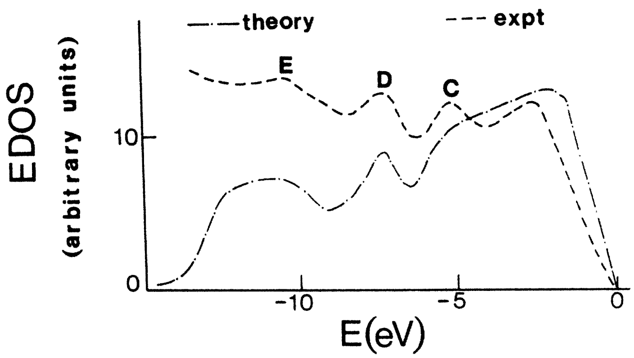

FIG. 5. The averaged total EDOS of two network models is compared with UPS data

tion exists between the changes in the Si-dominated vibrational modes and the local environment at the Si site which is neighboring to the removal H atom. The critical value of the distortion is about 5%. Similar results have been obtained from other cases.

B. Electronic properties

The total averaged EDOS for the two network models is shown as the dashed-dotted curve in Fig. 5. The photoemission data measured by von Roedern *et al.*[3] are shown as a dashed curve. The calculated peaks at -2.7, -7.5, and -10.5 eV agree well with the experimental results. There is a peak at -5.2 eV in the measurement, while the theory shows a shoulder at -5.0 eV.

As mentioned in Ref. 8, it is rather difficult to unambiguously calculate the H-related local DOS (LDOS) in the supercell approach. The results in Ref. 8 show four peaks at -11.5, -7.5, -5.0, and -2.0 eV. By removing H atoms and comparing the changes in the EDOS, we found a better way to determine the energies for the Si—H bonding states. In Fig. 6 we plot the total DOS with (a) all six H atoms in the network, (b) H(1) removed, (c) H(2) removed, and (d) H(3) removed. We find that, besides the states appearing at an average of 0.2 eV above the top of the VB, which are the dangling-bond states, the largest changes occur around -5.0 eV. The next most affected region is about -7.5 eV. The -10.5-eV structure remains unchanged. Therefore, we attribute the -7.5- and -5.0-eV regions to the H-atom related structures. For further proof we calculated the charge densities in the H(1)—Si(32)—Si(33) plane by (i) surrounding the H atom by a Voronoi polyhedron with its volume equal to $(1.48/2.35)^3$, where the quantity in the parentheses is the ratio of the Si—H and Si—Si bond lengths; (ii) calculated the probability

$$p_n = \rho_{\text{polyhedron}} \psi_n^2 d^3 r \tag{3}$$

for the nth state; (iii) calculated the charge density

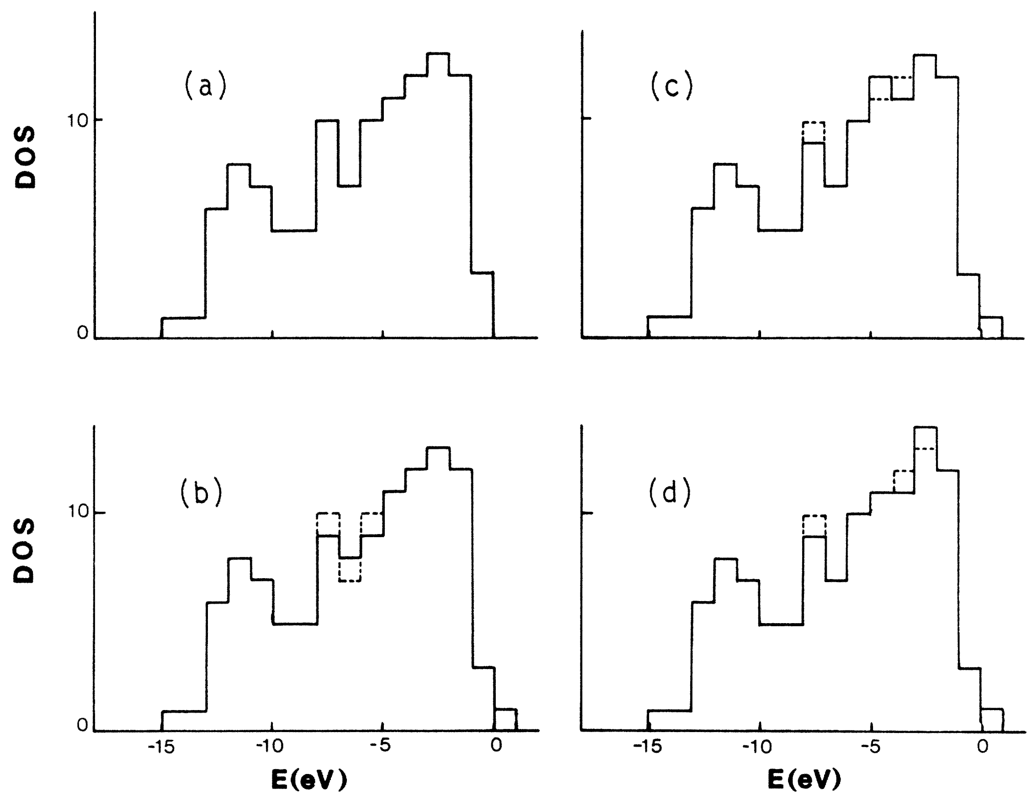

FIG. 6. (a) Total electronic density of states of one model serves as reference. (b) H(1) removed (solid line), the reference is shown as a dashed line. (c) H(2) removed (solid line). (d) H(3) removed (solid line).

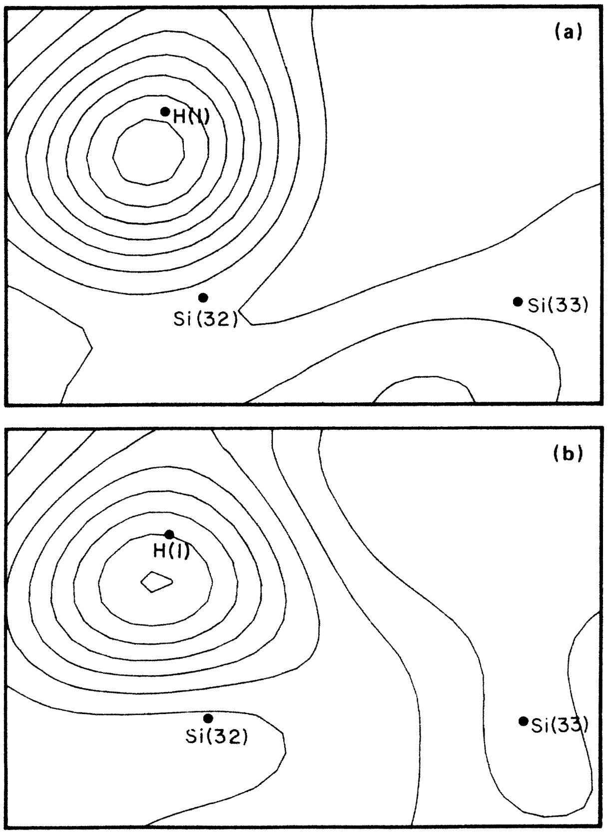

FIG. 7. (a) Charge density at H(1) associated with the -7.5-eV maximum. (b) Charge density at H(1) associated with the -5.0-eV maximum.

$$\rho(\bar{r})=\sum_n \rho_n(\bar{r})p_n \ , \quad (4)$$

where the sum is over states lying in the energy range of interest. Due to the weighting, only those states with large LDOS around H(1) will contribute. Consequently, the bond charges between Si(32) and Si(33) do not appear in Figs. 7(a) and 7(b). In Fig. 7(a) the charge density associated with the -7.5-eV structure is plotted. Most of the charge is concentrated at the H atom. However, the maximum of the charge is displaced from the H atom toward the Si(32). The contours are rather spherical, as expect for H 1s and Si 3s bonds. The charge density shown in Fig. 7(b) is associated with the -5.0-eV shoulder. At Si(32) there is essentially no charge density, indicating that mainly Si p states are contributing. The maximum of the charge is at the same distance from H(1) as the one shown in Fig. 7(a). This indicates that the charge distribution for this region is contributed from H 1s and Si 3p states.

The charge densities in the plane [H(1)—Si(32)—Si(33)] [Figs. 7(a) and 7(b)] can further be used to demonstrate the effect of local distortions on the charge distribution. For example, the maximum charge density in Fig. 7(a) is not along the H(1)—Si(32) bond direction. The bond angle at Si(32) is only 99.8°. Consequently, there is a stronger Coulomb repulsion between the bond charges along H(1)—Si(32) and those along Si(32)—Si(33) compared to the case where the angle has the ideal value of 109°. Therefore, the maximum of the charge density for H(1)—Si(32) is shifted away from H(1)—Si(32) bonds direction. A similar displacement of maximum charge density is also seen in Fig. 7(b). Table IV summarizes the comparison between the present results and previous studies.

Finally, we discuss the dangling bond states associated with threefold coordinated Si atoms. As mentioned earlier, we found that the dangling-bond states are at an average of 0.2 eV above the energy of the top of the VB (E_v). The three cases are at $E_v+0.01$, 0.2, and 0.45 eV, so that, as one would expect, fluctuations in the environments of the threefold coordinated atom cause their energies to form a band. The average of the calculated value is closer to the VB edge than the experimentally measured energy of the T_3^0 level (g factor $=2.0055$) at $E_v+0.7$ eV at a spin density of 10^{17} cm^{-3}.[22] This energy is determined from the doped a-Si:H samples. Unfortunately, the energy of the dangling bond has not been measured for undoped sample. Recently, Adler *et al.*[23] estimated the value at $E_v+0.5$ eV. The determination of the energies of the dangling-bond states is complicated by other difficulties, such as uncertainty in the position of E_v when dealing with only a few states, or discriminating between the energy of a single defect state and that of the two or more nearby defects. The discrepancy between the present theoretical results and

TABLE IV. Comparison of experimental and theoretical results in Si—H bonding states.

Binding energy (eV) of monohydride		Method	Reference
C peak	D peak		
5.2	7.4	UPS (experimental)	3
7.0	10.0	LCAO-cluster	7
5.0		CBL	9
4.5		Self-consistent CBL	10
5.2	7.6	Coherent potential approximation	11
5.0		Tight-binding	21
5.0	7.5	Self-consistent pseudopotential	present work

the generally accepted energy of the dangling bond may only be resolved by future experimental data on undoped a-Si:H. As a parallel to the vibrational calculations, we present the charge distributions in the same plane as in Fig. 7 for three typical situations: (1) H(1) removed (one dangling bond present), (ii) H(1) and H(2) removed (two dangling bonds present, but not sharing a common second neighbor), (iii) H(1) and H(3) removed (two dangling bonds present, and sharing a common second neighbor). These three situations enable us to correlate the orientation of the charge distributions for the dangling-bond states with its local environment, and to estimate the range of interaction between the dangling bonds. In Fig. 8(a) we plot the charge density around H(1) for reference. Again, the bond charge between Si(32) and Si(33) is absent because of the weighting scheme given in Eqs. (3) and (4). When H(1) is removed [Fig. 8(b)], the maximum of the charge density moved closer to Si(32) and away from the Si(32)—Si(33) bond. This change allows the dangling bond to minimize the Coulomb interactions with its local environment, and to move closer to the ideal tetrahedral bond angle. [Recall that the bond angle at Si(32) with H(1) present was only 99.8°.] This result clearly shows that local distortions can have a significant effect on the orientation of the dangling bond. Studies of dangling bonds with ideal geometrical configurations may thus be unrealistic. The results corresponding to the removal of both H(1) and H(2) is depicted in Fig. 8(c). The charge distribution around H(1) exhibits the same qualitative features as those in Fig. 8(b), indicating that H(1) and H(2) are far enough apart so that they do not interact.

In Fig. 8(d) we give a contour plot around H(1) with both H(1) and H(3) removed. The changes with respect to the results in Fig. 8(b) can be easily discerned. One feature is the movement of charge into the open region in Fig. 8(b). These results suggest that dangling bonds can interact if they share a common second neighbor.

In summary, we have studied the effects of removing H atoms on the vibrational and the electronic properties of a-Si:H. For the vibrational properties, the removal of H can induce changes in the low-frequency Si-dominant modes. Our results are consistent with the recent Raman scattering experiments in a-$Si_{1-x}H_x$ (Ref. 24) which also show changes in the low-frequency TA and LA bands with x. We demonstrate also the strong correlations between the changes and the local environments.

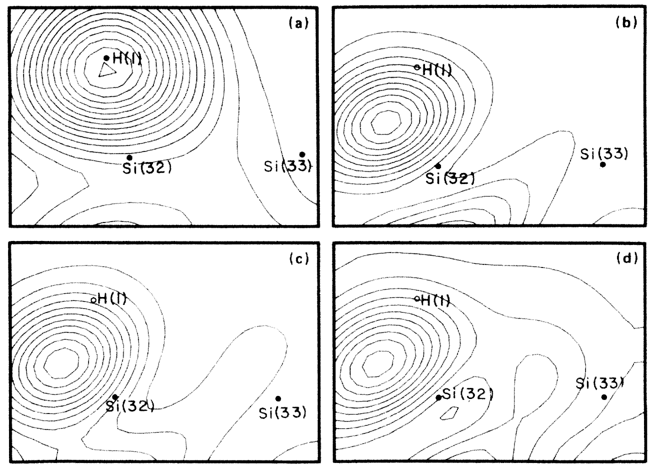

FIG. 8. (a) Total charge density at H(1) in H(1)—Si(32)—Si(33) plane. (b) H(1) removed–the dangling bond charge density. (c) H(1)—Si(32)—Si(33) plane with H(1) and H(2) removed. (d) H(1)—Si(32)—Si(33) plane with the H(1) and H(3) removed.

For the electronic properties, we have used the variations in electronic DOS caused by the removal of H atoms to identify the H—Si bonding states. Furthermore, the properties of the dangling bond have been calculated. From the charge distributions of the dangling bonds, the importance of the local environment is also clearly manifested. So, the models provide useful information of correlations between the physical properties and the local environments in a-Si:H.

An unexpected outcome from our studies is that the interaction range between the bond charges and the ions is the same ($\lesssim 4$ Å), even though the former was treated by the self-consistent scheme and the latter was studied by an explicit second-neighbor potential. It is the screening effect which reduces the range of interaction between the bond charges. Our calculations justify the application of the tight-binding method with short-range interactions to a-Si.

ACKNOWLEDGMENT

One of us (L.G.) is supported by the U.S. Department of Energy. We would like to thank C. S. Nichols for a critical reading of the manuscript.

[1]W. Paul, A. J. Lewis, G. A. N. Connell, and T. D. Moustakas, Solid State Commun. **20**, 969 (1976).

[2]S. C. Shen, C. J. Fang, M. Cardona, and L. Genzel, Phys. Rev. B **22**, 2913 (1980).

[3]B. von Roedern, L. Ley, M. Cardona, and F. W. Smith, Philos. Mag. B **40**, 433 (1979).

[4]R. A. Barrio, L. E. Sansores, and R. J. Elliott, J. Non-Cryst. Solids **59&60**, 177 (1983).

[5]M. F. Ross, C. M. Perlov, C. Y. Fong, and L. Guttman, J. Non-Cryst. Solids **59&60**, 209 (1983).

[6]K. Winer and F. Wooten, J. Non-Cryst. Solids **59&60**, 193 (1983); K. Winer and F. Wooten, Phys. Status Solidi B **124**, 473 (1984).

[7]W. Y. Ching, D. J. Lam, and C. C. Lin, Phys. Rev. Lett. **42**, 805 (1979); W. Y. Ching, D. J. Lam and C. C. Lin, Phys. Rev. B **21**, 2378 (1980).

[8]C. Y. Fong and L. Guttman, in *Tetrahedrally Bonded Amorphous Semiconductors (Carefree, AZ, 1981)*, Proceedings of the Conference on Tetrahedrally Bonded Semiconductors, AIP Conf. Proc. No. 73, edited by R. A. Street, D. K.

Biegelsen, and J. C. Knights (AIP, New York, 1981), p. 125; L. Guttman and C. Y. Fong, Phys. Rev. B **26**, 6756 (1982).

[9]D. C. Allan and J D Joannopoulos, J. Non-Cryst. Solids **59&60**, 136 (1981); D. C. Allan, J. D. Joannopoulos and W. B. Pollard, Phys. Rev. B **25**, 1065 (1982).

[10]G. Diaz, E. Martinez, and F. Yńdurain, Phys. Rev. Lett. **56**, 1731 (1986).

[11]E. N. Economou and D. A. Papaconstantopoulos, Phys. Rev. B **23**, 2042 (1981).

[12]J. S. Nelson, C. Y. Fong, L. Guttman, and I. P. Batra, J. Non-Cryst. Solids **77&78**, 1109 (1985).

[13]L. Guttman, Phys. Rev. B **23**, 1866 (1981).

[14]P. N. Keating, Phys. Rev. **145**, 637 (1966).

[15]R. M. Martin, Phys. Rev. B **1**, 4005 (1970).

[16]J. C. Knights, G. Lucovsky, and R. J. Nemanich, Philos. Mag. B **37**, 467 (1978).

[17]K. M. Ho, M. L. Cohen, and M. Schlüter, Phys. Rev. B **15**, 3888 (1977).

[18]W. A. Kamitakahara, H. R. Shanks, J. F. McClelland, U. Buchenau, F. Gomf, and L. Pintschovius, Phys. Rev. Lett. **52**, 644 (1984).

[19]C. S. Nichols, M. F. Ross, and C. Y. Fong, Phys. Rev. B **32**, 1061 (1985).

[20]O. Imagawa, M. Iwanishi, S. Yokoyama, and K. Shimakawa, J. Non-Cryst. Solids **77&78**, 359 (1985).

[21]K. C. Pandey, T. Sakurai, and H. D. Hagstrum, Phys. Rev. Lett. **35**, 1728 (1975).

[22]R. A. Street and D. K. Biegelsen, in *The Physics of Hydrogenated Amorphous Silicon II,* edited by J. D. Joannopoulos and G. Lucovsky (Springer-Verlag, Berlin, 1984), p. 195; H. Dersch, J. Stuke, and J. Beichler, Phys. Status Solidi B **105**, 265 (1981).

[23]D. Adler, M. Silver, M. P. Shaw, and V. Cannella, in *Materials in Amorphous-Semiconductor Technology,* edited by D. Adler, Y. Hamakawa, and A. Madan (Materials Research Society, Pittsburgh, 1986), p. 113.

[24]N. Maley and J. S. Lannin, Bull. Am. Phys. Soc. **32**, 634 (1987).